Resistance of young gelatinase B–deficient mice to experimental autoimmune encephalomyelitis and necrotizing tail lesions

Bénédicte Dubois,[1] Stefan Masure,[1] Ursula Hurtenbach,[2] Liesbet Paemen,[1] Hubertine Heremans,[1] Joost van den Oord,[3] Raf Sciot,[4] Thorsten Meinhardt,[2] Günter Hämmerling,[2] Ghislain Opdenakker,[1] and Bernd Arnold[2]

[1]Rega Institute for Medical Research, University of Leuven, B-3000 Leuven, Belgium
[2]Laboratory of Molecular Immunology, German Cancer Research Center, D69120 Heidelberg, Germany
[3]Laboratory of Histo- and Cytochemistry, and
[4]Laboratory of Neuropathology, University of Leuven, B3000 Leuven, Belgium

Address correspondence to: G. Opdenakker, Rega Institute for Medical Research, Laboratory of Molecular Immunology, Minderbroedersstraat 10, B-3000 Leuven, Belgium. Phone: 32-16-337385; Fax: 32-16-337340; E-mail: Ghislain.Opdenakker@rega.kuleuven.ac.be.

Bénédicte Dubois and Stefan Masure contributed equally to this work.

Received for publication March 23, 1999, and accepted in revised form October 18, 1999.

Regulated expression of matrix metalloproteinases (MMPs) and their inhibitors (TIMPs) plays a role in various physiological processes. To determine in vivo how unbalanced expression of these factors can promote or affect the course of pathologies, we knocked out the mouse gelatinase B gene by replacing the catalytic and zinc-binding domains with an antisense-oriented neomycin resistance gene. Adult gelatinase B–deficient mice and wild-type controls could be induced to develop experimental autoimmune encephalomyelitis (EAE) with similar scores for neurologic disease, blood-brain barrier permeability, and central nervous system histopathology. However, whereas diseased control animals showed necrotizing tail lesions with hyperplasia of osteocartilaginous tissue, adult gelatinase B–deficient mice were resistant to this tail pathology. Gelatinase B–deficient mice younger than 4 weeks of age were significantly less susceptible to the development of EAE than were age matched controls and, even as they aged, they remained resistant to tail lesions. These data illustrate that gelatinase B expression plays a role in the development of the immune system and that, in ontogenesis, the propensity to develop autoimmunity is altered by the absence of this MMP.

J. Clin. Invest. **104**:1507–1515 (1999).

Introduction

Matrix metalloproteinases (MMPs) are involved in various physiological (1–5) as well as pathological (6–17) processes. Gelatinases belong to the secreted matrix metalloproteinases and constitute a terminal step in the enzyme cascade that processes extracellular matrices including basement membranes (18–20). Two types are distinguished: gelatinase A (MMP-2) and gelatinase B (MMP-9) (Figure 1a). The former has a molecular weight of 65–75 kDa, lacks a collagen-like domain and is, in general, constitutively present in all body fluids. The latter is inducible and has a molecular weight of more than 85 kDa. The MMPs are synthesized as zymogen-like latent precursors and are converted subsequently to the active form of the zinc proteases by the cysteine switch mechanism (21). In terms of protein and domain structure, gelatinase B is the largest and most complex member identified so far. From in vitro studies, it has been deduced that gelatinase B expression is characterized by a complex regulation with tight control at several levels, e.g., gene transcription and protein secretion by cytokines and chemokines (8, 19, 22–24), action of tissue inhibitors of matrix metalloproteinases (TIMPs) (18, 25, 26), and proenzyme activation by components of the plasminogen activation system (19, 20, 22, 27) or other MMPs (28).

The possible functions of this enzyme cascade, including gelatinase B, in central nervous system (CNS) inflammation may be manifold (19, 22, 29): cleavage of myelin proteins (30–32), degradation of collagen IV in the basement membranes (33, 34), activation or degradation of disease-modifying cytokines (35), and direct damage of CNS cells.

Gelatinase B has been detected in the cerebrospinal fluid of patients with optic neuritis, multiple sclerosis (MS), and other inflammatory neurologic diseases, but not in normal control patients, whereas gelatinase A was constitutively present in all samples (10, 11). Immunohistochemical reaction with gelatinase B–specific mAb's (36) was documented within human MS plaques in concert with the expression of other metallo- and serine proteases and specific inhibitors (13).

Experimental autoimmune encephalomyelitis (EAE) is used as an animal model for MS. However, there exist many variants of EAE depending on the animal species

(rat, mouse, primates), the inducing agent (microbial or myelin components, spinal cord homogenates, adoptive transfer of specific T-cell clones), and the clinical course (acute, chronic with relapses) (37, 38). In mouse EAE, gelatinase B was increased in the cerebrospinal fluid of diseased mice (31). Recently, it was demonstrated that levels of MMP-9 mRNA were increased in adoptive transfer EAE at times of maximum disease severity. Positive immunochemical staining with an MMP-9–specific mAb was observed along the meninges, around blood vessels, and within the parenchyma in diseased but not in normal animals (39). Biochemical (30, 31), histological, and immunochemical (13) studies, as well as EAE experiments in which protease inhibitors were used (40–45), illustrate that CNS inflammation is mediated by proteases. The disease-limiting effects of protease inhibitors are indicative of a role for serine proteases or MMPs in EAE. Finally, the beneficial effect of IFN-β on MS may be mediated by a control of the protease balance, the net activity of proteases and protease inhibitors (19), e.g., by an inhibition of the gelatinase B expression resulting in a reduction of T-lymphocyte infiltration into the CNS (46, 47).

All of these elements constitute indirect evidence for a role for gelatinase B in the damage caused by inflammation and demyelination in the CNS. In this study, gelatinase B–deficient mice were generated, and the clinical and histopathological effects of gelatinase B action were compared in wild-type versus knockout mice in a specific model of EAE.

Methods

Construction of targeting vector pPNT/mGEL-B and generation of gelatinase B–deficient mice. Figure 1a compares the protein domain structures of gelatinase A and B and indicates the positions of the coding regions of each domain in the mouse gelatinase B gene, which was fully characterized (48) by Masure et al. (EMBL accession number X72794). From the cosmid clone MMG1, subclones were derived and additional (5 kilobase pair [kbp] upstream and 5 kbp downstream) nucleotide sequences were determined. A targeting vector pPNT/mGEL-B (Figure 1b) was constructed in pUC19 with the herpes simplex virus (HSV) thymidine kinase (TK) gene in front of the mouse gelatinase B gene, in which the exons and corresponding introns 3–7 and about half of exon 8 (2,067 bp total) were deleted and replaced by the neomycine resistance gene (NEO; 1,840 bp). pPNT/mGEL-B was generated by cloning an approximately 5.5-kbp *Kpn*I-*Bam*HI fragment of the cosmid clone MMG1 (starting at the *Kpn*I site, which is 4 kbp upstream of the transcription start and extending to the *Bam*HI site in intron 2–3) into pPNT/*Kpn*I-*Bam*HI in between the TK gene (5′-end) and the NEO gene (3′-end). The orientation of the gelatinase B gene segments is antisense compared with TK and NEO. Next, a 5,200-bp *Xho*I-*Bgl*II fragment was isolated from cosmid MMG1. This fragment contains the second half of exon 8 and exons 9–13, plus the corresponding introns and 1.5 kbp of the 3′-untranslated region of the gelatinase B gene. This fragment was first subcloned in pBluescript/*Xho*I-*Bam*HI and subsequently transferred as a *Xho*I-*Not*I fragment into the aforementioned pPNT-derivative. The resulting targeting vector is 18,061 bp and contains 10.7 kbp of the mouse gelatinase B gene in which the deleted parts are most of the catalytic domain (exons 3–4) and the zinc-binding domain (exon 8). The latter 2 domains are essential for enzymatic activity, and homologous recombination should result in complete lack of gelatinase B activity in homozygote knockout animals. Twenty micrograms of the targeting vector was digested to linear fragments with *NotI* and electroporated into 10^7 E14-J embryonic stem (ES) cells. Homologous recombination events were identified by Southern analysis using external probes. ES cells from 3 positive clones were injected into C57BL/6 blastocysts to generate chimeric mice. All animals were kept in a specific pathogen–free (SPF) environment. The first generations were monitored by Southern blot analysis (Figure 1c). As the numbers of animals increased, a PCR-based method was developed (Figure 1d) for fast screening. The following primer combinations were used: gAAgCAgCgACTAgggATTgTggg and ACAggCATACTTgTACCgCTATgg for detection of the wild-type allele, the latter primer, and AACgAgATCAgCAgCCTCTgTTCC for the knockout allele. To confirm that the results were not strain dependent, selected studies were done with homozygous gelatinase B–deficient and wild-type littermates and descendants from the crosses between heterozygous mice. Moreover, when C57Bl/6 controls were compared with wild-type mice from crosses between heterozygous animals, no differences in EAE and tail pathology were observed.

Induction of acute EAE in mice. All in vivo experimental and ex vivo sampling protocols were approved by the Animal Welfare Board of the Ministry of Agriculture (certification: LA 1210243, Belgium) and the Ethical Committee of the Medical Faculty of the University of Leuven.

Acute EAE was induced by injection of 50 μL of sonicated emulsion consisting of 100 mg/mL lyophilized spinal cord homogenate (from the SJL mouse strain) in PBS and 4 mg/mL heat-killed *Mycobacterium tuberculosis* (strain H37Ra) in CFA (both reagents from Difco Laboratories, Detroit, Michigan, USA). The injection was performed in each hind footpad on day 0. On day 0 and day 2 or 3, 50 μL of *Bordetella pertussis* vaccine (10^{10} cells; kind gift of R.H. Tiesjema, Rijksinstituut voor de Volksgezondheid, RIV, Bilthoven, the Netherlands) was intravenously administered in the tail vein. Animals were ether anesthetized for the subcutaneous injection.

The animals were kept on a 15-hour–light/9-hour-dark cycle under SPF conditions to avoid interference with contaminating pathogens. They were manipulated with gloves under laminar air flow. Each day and throughout the experiments, they were evaluated by the same observer. The disease and mortality were scored on a scale of 0–6, as described elsewhere (49): 0 = normal; 0.5 = flop-

py tail; 1 = tail paralysis and mild impaired righting reflex; 2 = mild hind limb weakness and impaired righting reflex; 3 = moderate to severe hind limb paresis and/or forelimb weakness; and 4 = hind leg paralysis and/or moderate to severe forelimb weakness; 5 = quadriplegia or moribund; 6 = death. Food was placed on the cage floor, and the animals were provided with a long drinking tube to exclude malnutrition and dehydration due to limb paralysis.

Degranulation of leukocytes and detection of gelatinase activity. Heparinized blood samples were obtained by performing a heart puncture in ether-anesthetized animals. The blood was cooled on ice, and after cen trifugation (1000 *g* for 10 minutes at 4°C), the cells were washed by PBS. The centrifugation step was repeated. The cells were resuspended and incubated overnight at 37°C, 5% CO_2 in 100 µL serum-free medium supplemented with phorbol-12-myristate-13-acetate in a final concentration of 100 ng/mL to stimulate degranulation of neutrophils. Then, the cells were pelleted and the supernatant was frozen at –20°C until analysis. Gelatinase activity was determined by SDS/PAGE zymography as described previously (23).

Histology. The autopsies were performed at different stages of EAE development, both in the knockout and in the wild-type mice. The animals were sacrificed by ether anesthesia, and a heart puncture was done to collect leukocytes and to exsanguinate the animals. The spinal cord was removed immediately, divided in 3 parts (cervical, thoracic, and lumbosacral spinal cord) and fixed in formalin (6%). This material was paraffin embedded, and 4-µm sections were cut. They were routinely stained with hematoxylin and eosin and by a Klüver-Barrera stain. Histopathology was assessed as follows. Several sections of the 3 parts (cervical, thoracic, lumbosacral) of the spinal cord were evaluated. A global inflammatory score was given to each part as follows: 0 = normal; 1 = presence of a perivascular inflammatory cuff; 2 = circumferential presence of inflammatory cell groups around the spinal cord; and 3 = circumferential inflammation with parenchymal invasion. A mean inflammatory score was defined as the sum of all read-outs, divided by the number of analyzed dissected parts. Furthermore, the predominance of mononuclear or polymorphonuclear cells was assessed in each of the 3 parts of the spinal cord.

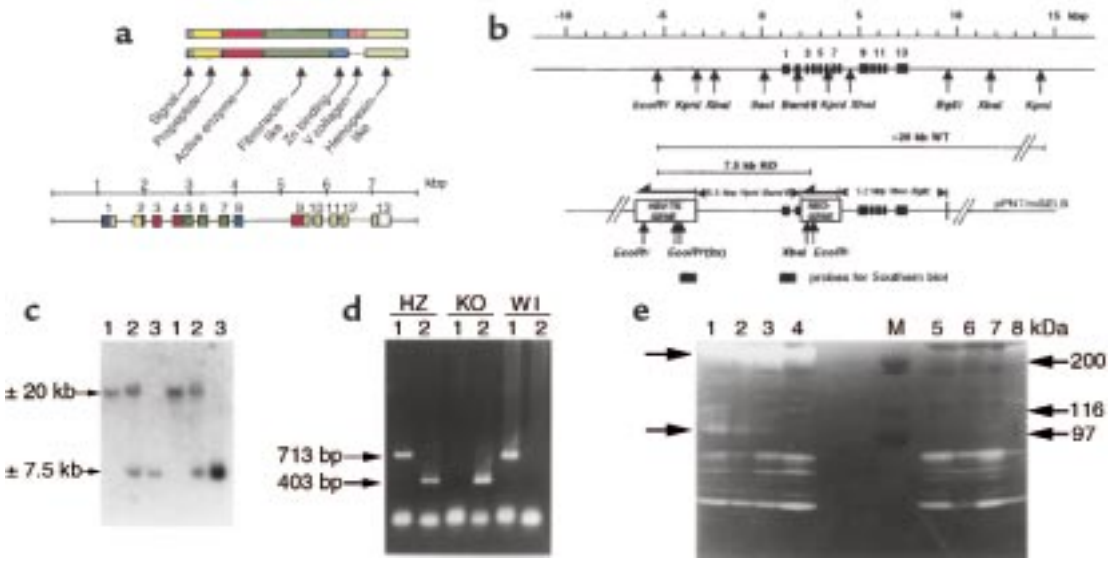

Figure 1
Generation of gelatinase B–deficient mice. (**a**) Gelatinase A and B protein domain structure and gene organization of gelatinase B. Gelatinase B contains a type V collagen-like domain, not present in gelatinase A. Each domain is named, and a color code is used to indicate within the mouse genomic structure the exon parts that encode the respective protein domains. (**b**) Construction of targeting vector pPNT/mGEL-B. The sequence of the mouse gelatinase B gene (accession number X72794) was extended at the 5′- and 3′-ends, and fragments from the wild-type gene were used to generate the targeting vector pPNT/mGEL-B. Representative restriction sites for subcloning and analysis of wild-type or homologously recombined knockout genes are indicated. The scale bar indicates the fragment sizes in kbp. The orientation of the HSV-TK and NEO genes are antisense to the gelatinase B gene segments as indicated by the arrows. The localization of the 5′-end probes, used for Southern blot analysis, is indicated. (**c**) Genotyping by Southern blot analysis. Hybridization of EcoRV-digested tail DNA with a 5′-end probe resulted in bands of approximately 20 kb or 7.5 kb. Lanes 1 show the hybridization patterns of genomic DNA from wild-type mice, whereas lanes 2 are from heterozygote, and lanes 3 from gelatinase B–deficient, mice. (**d**) Screening by PCR analysis. Lanes 1 indicate the results of PCR, performed with a primer set to view the wild-type allele. Lanes 2 show the reaction products obtained with a knockout-specific primer set. The resulting genotype is indicated by heterozygous (HZ), knockout (KO), and wild-type (WT). The sizes of the amplified DNA-fragments are indicated in basepairs. (**e**) Functional analysis by zymography. Gelatinase activity was determined by SDS/PAGE gelatin substrate conversion. Lanes 1–4 show the analysis of leukocyte supernatants of 4 individual wild-type mice; lanes 5–8, those of 4 gelatinase B–deficient mice. The arrows indicate the gelatinase B zymolysis. Similar to control preparations of recombinant mouse gelatinase B, this zymolysis occurs mainly at >200 kDa (dimer, solid arrow), but also at the monomer position (110 kDa, arrowhead). M, molecular weight standardization.

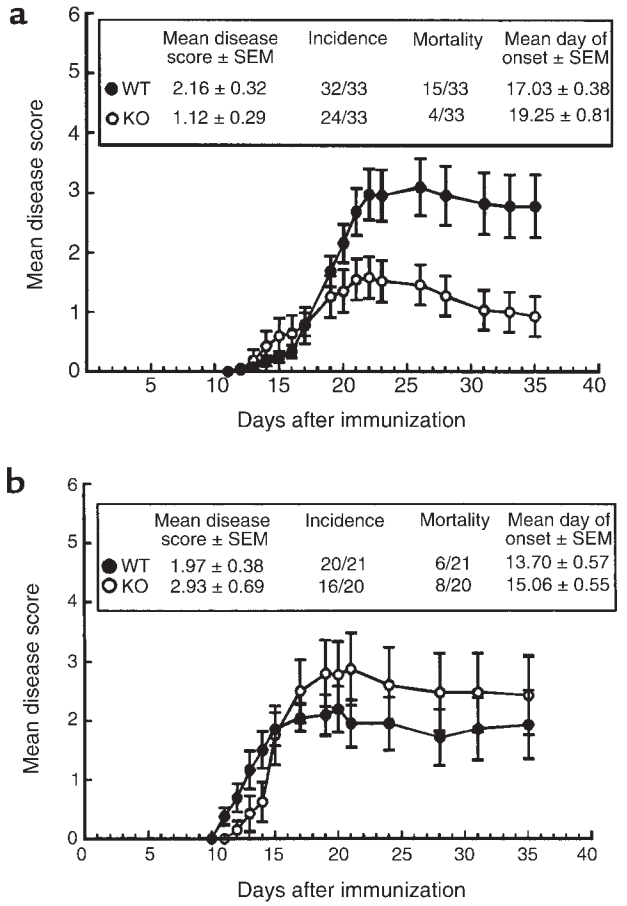

Figure 2
Induction of acute EAE in gelatinase B–deficient and wild-type mice. (**a**) Groups of 3- to 4-week-old mice were immunized with SJL-spinal cord homogenates to develop EAE. Mean disease score, mean day of onset, incidence, and mortality (insets) were calculated on the pooled data of 3 independent experiments. Dead animals were scored 6 from the day of death until the end of the study. (**b**) EAE was induced in adult (7- to 8-week-old) gelatinase B–deficient and wild-type mice. The insets show the disease parameters that were calculated on the pooled data of 2 experiments.

Blood-brain barrier permeability. Permeability of the blood-brain barrier was analyzed as described previously (42). Mice were injected intravenously with 1% (wt/vol) Evans blue (Sigma-Aldrich, Bornem, Belgium) in PBS at a dosage of 5 μL/g body weight. After 1 hour, the animals were sacrificed by CO_2 inhalation and perfused with PBS via the left ventricle. The CNS was dissected and divided in 3 parts: the spinal cord, the cerebellum with the brainstem, and the cerebrum. Each part was weighted, and tissue samples were then extracted for 3 days in formamide (5 μL/mg tissue). The extracts were centrifuged for 5 minutes at 500 *g*. Evans blue concentration was determined for each extract separately by measuring the absorbance at 650 nm. In addition, a pool of the extracts of the whole CNS was made. Two different permeability indices were calculated: the A_{650} ratio of knockout versus wild-type animals (in diseased and in noninduced animals), and the A_{650} ratio of diseased versus normal mice (in knockout and wild-type animals). These analyses were performed in young as well as in adult animals.

Statistical analysis. The mean disease score was defined as the mean of all individual daily scores from the day on which the first symptoms appeared until day 35 (included). For statistical analysis of the mean disease score and the mean day of onset, the Wilcoxon test was used. Significance of differences in EAE incidence and mortality between the gelatinase B–deficient and the wild-type mice was calculated by the χ^2 method with the correction of Yates. Dead animals were scored 6 from the day of death until the end of the study.

Differences in blood-brain barrier permeability were assessed using the Wilcoxon test. This test was also used to analyze the differences in inflammation scores. Differences in mononuclear or polymorphonuclear cell predominance were evaluated by the χ^2 method with Yates' correction. Values of $P \leq 0.05$ were defined as statistically significant.

Results

Generation of gelatinase B–deficient mice. A targeting vector pPNT/mGEL-B was constructed in which the essential segments of the mouse gene (48), coding for the enzymatic activity of gelatinase B, were deleted and replaced by an antisense-oriented neomycin resistance gene (Figure 1b). The vector pPNT/mGELB was injected into ES cells, and the blastocysts were implanted in pseudo-pregnant mice. Ten chimeras derived from 3 independent ES cell lines transmitted the disrupted MMP-9 gene through the germline as shown by Southern blot analysis. Matings of heterozygous mice resulted in the expected mendelian frequency of MMP-$9^{-/-}$ (81/359, 22.6%), MMP-$9^{+/-}$ (177/359, 49.3%), and MMP-$9^{+/+}$ (101/359, 28.1%) mice, suggesting that embryonic and fetal development of homozygous mutant mice were not impaired. Further inbreeding and genotyping (Figure 1, c and d) yielded the gelatinase B–deficient animals and controls used in this study. During a follow-up period of more than 3 years, gelatinase B–deficient mice did not show gross phenotypic abnormalities, nor histopathological changes in parenchymatous organs when compared with wild-type animals. Both wild-type and gelatinase B–deficient mice appeared normal, and there was no difference in viability.

Expression of gelatinase B. To verify the gelatinase status in control and knockout mice, gelatinases were analyzed by zymography. Peripheral blood leukocytes were collected from individual wild-type and gelatinase B–deficient mice, purified, and stimulated with phorbol ester. As is clear from the zymography, shown in Figure 1e, leukocytes from gelatinase B–deficient mice did not express gelatinase B, in contrast to their wild-type controls, in which substantial levels of gelatinase B activity are present. As an internal control for sample preparation and handling, all samples contained constitutive gelatinases. From the zymography analysis, we could deduce that the deficiency in gelatinase B was not quantitatively compensated for by increased levels of other gelatinases.

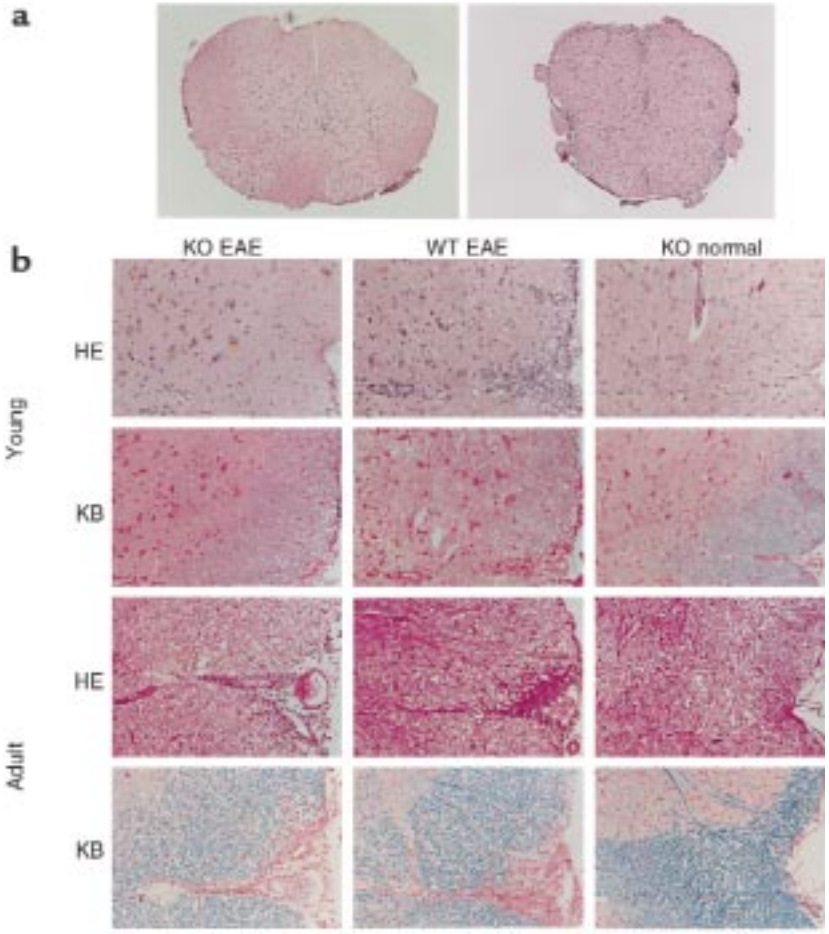

Figure 3
Neuropathological findings in gelatinase B–deficient mice with EAE. (**a**) Shows different inflammation stages (stage 1, left; stage 3, right) on the basis of which the inflammatory score was calculated. ×42. (**b**) Shows hematoxylin-eosin (HE) and Klüver-Barrera (KB) stains of the spinal cord of young and adult gelatinase B–deficient (KO) or wild-type (WT) mice in a diseased (EAE) or in a normal state. ×110. The histology in normal wild-type mice was similar to that of gelatinase B–deficient animals.

Resistance to development of EAE in young gelatinase B–deficient mice. Because we did not observe a "spontaneous phenotype" in the gelatinase B–deficient mice, and as gelatinase B had previously been shown to be an inducible enzyme, we induced EAE and compared its clinical course in wild-type and gelatinase B–deficient mice. Clinical symptoms progressed in a caudal to rostral direction. The signs started with tail paralysis, which subsequently spread to the back limbs. The symptoms usually peaked with paralysis of the forelimbs. This was often followed by a remission that was, however, not always complete.

When EAE experiments were performed in 3- to 4-week-old mice, the disease course differed between gelatinase B–deficient and control mice. Three independent experiments (pooled data in Figure 2a) confirmed a lower susceptibility of these young gelatinase B–deficient mice to EAE when compared with age-matched wild-types. Statistical analysis yielded significant differences for the mean disease score ($P = 0.02$), mortality ($P = 0.007$), incidence of disease ($P = 0.02$), and mean day of onset ($P = 0.02$).

Susceptibility to EAE in adult gelatinase B–deficient mice. EAE was also induced in adult (7- to 8-week-old) gelatinase B–deficient and wild-type mice (Figure 2b). Statistical analysis on the pooled data from Figure 2b yielded no differences between gelatinase B–deficient and wild-type mice. Mean disease score ($P = 0.44$), mortality ($P = 0.58$), and incidence of disease ($P = 0.31$) did not differ significantly between both groups. However, disease tended to start later in the knockout mice ($P = 0.07$).

Histopathology: inflammation and demyelination assessment. An extensive histopathological comparison of the CNS lesions was made between young as well as adult gelatinase B–deficient and control mice and scored as outlined in Methods (Figure 3a). In young gelatinase B–deficient mice the inflammatory score (mean value = 1.29) of each spinal cord part ($n = 35$) was significantly lower ($P = 0.0015$) than that of the wild-type controls (mean value = 2.44; $n = 18$) (Figure 3b). In the knockout mice, the inflammatory infiltrates consisted of less polymorphonuclear cells ($P = 0.003$), whereas the presence of mononuclear cells was equivalent in both groups ($P = 0.94$). In the adult animals (Figure 3b), similar analyses did not yield significant differences between knockout and wild-type mice. For instance, the inflammatory score was not different in gelatinase B–deficient mice (mean value = 1.69; $n = 26$) compared with wild-type animals (mean value = 1.58; $n = 24$). Mononuclear cells and neutrophils were equally distributed in both groups of adult mice (mononuclear cells: $P = 0.91$; polymorphonuclear cells: $P = 0.31$). No signs of demyelination were observed within the experimental period of 26 days (Klüver-Barrera stains in Figure 3b).

Figure 4
Tail necrosis in wild-type animals. Various forms of tail necrosis were observed in wild-type animals: loss of necrotic tail end (upper panel) and ulceration and subsequent necrosis (middle) leading to amputation with blunt end (lower panel).

Blood-brain barrier permeability. Table 1 summarizes the results of experiments that were performed to assess the blood-brain barrier permeability. Intravenous injection of Evans blue resulted in equivalent staining of the CNS in diseased knockout and wild-type mice, both in the young and in the adult animals. In contrast, the blood-brain barrier permeability increased consistently in mice that developed EAE symptoms compared with healthy controls. Because the overall permeability of the entire CNS was lower than that of the spinal cord, the results are in line with an ascending damage of the blood-brain barrier in EAE. This observation is in accordance with the neurological symptoms of an ascending myelitis. Although the A_{650} ratios observed in the young gelatinase B–deficient mice (1.85 and 1.44) do not reach the level of significance, they appear to be very close to the values in adult mice (2.00 and 1.39). These small differences were strengthened by observations in a further experiment in which the blood-brain barrier permeability in young knockout animals that were resistant to the development of EAE was compared with that of normal (noninduced) gelatinase B–deficient mice. In this case, a mean value of A_{650} ratio (EAE-resistant KO/control KO) was found to be 1.33 (P = 0.02) for the total CNS. This implies that EAE-induction per se damages the blood-brain barrier, even without the development of clinical signs. As expected, when overt clinical disease develops, these ratios increase up to a value of about 2.00.

Necrotizing tail lesions. In young animals, 28 of 33 wild-type mice developed necrotizing lesions of the tail (Figure 4). In the gelatinase B–deficient mice, much less severe tail lesions were seen in only 13 of 33 animals. Statistical analysis between wild-type and gelatinase B–deficient mice, performed on the pooled data of 3 independent experiments, revealed a significant difference (P = 0.0005) for the incidence of tail lesions.

Similar results (P = 0.0002) were obtained for adult mice. Of 21 wild-type mice, 17 developed tail lesions. Only 3 knockout mice of 20 developed such lesions, which again were much less severe and usually healed.

In both age groups, the neurological disease score was not directly related to the occurrence of tail lesions, but neurologically nonaffected animals retained a healthy tail and the lesions appeared usually when the disease process was at its height.

The histopathology (Figure 5) of these tail lesions consisted in the earliest phase of an accumulation of eosinophilic fibrinoid material underneath the epidermis. This was accompanied by dilatation of small blood vessels, some edema, and a sparse inflammatory infiltrate in the superficial stroma of the dermis. Subsequently, the epidermis became increasingly thinner, ultimately resulting in complete ulceration and covering by a fibrinopurulent exudate. The adjacent, uninvolved epidermis showed reactive irregular hyperplasia. After ulceration, the osteocartilaginous tissue in the center of the tail showed pronounced hyperplasia, with many

Table 1
Blood-brain barrier permeability in gelatinase B–deficient mice

Compared groups[A]	Young mice		Adult mice	
	Spinal cord	Total CNS	Spinal cord	Total CNS
Control KO/control WT	0.93[B] (P = 0.66)[C]	1	1.27 (P = 0.04)	1.17 (P = 0.18)
Diseased KO/diseased WT	1.14 (P = 0.72)	1.08 (P = 0.72)	1.27 (P = 0.27)	1.14 (P = 0.24)
Diseased KO/control KO	1.85 (P = 0.17)	1.44 (P = 0.15)	2.00 (P = 0.008)	1.39 (P = 0.07)
Diseased WT/control WT	1.5 (P = 0.09)	1.36 (P = 0.05)	2.00 (P = 0.04)	1.43 (P = 0.07)

[A]Groups of at least 4 noninduced control and 10 diseased knockout (KO) or wild-type (WT) mice were compared. [B]Blood-brain permeability was assessed by intravenous injection of Evans blue and colorimetric determination in extracts of spinal cord or total CNS (42). Evans blue incorporation was calculated as the ratio of the mean value of the A_{650} of compared groups. [C]The distribution of the absolute A_{650} values of each sample in 1 group was compared with those of the other group, and the significance level was calculated.

irregular outgrowths of osseous tissue, in particular, underneath the ulceration. In some cases, this hyperplastic reaction resulted in extrusion of the osseous tissue through the ulceration (Figure 5). In addition, areas of chondroid tissue with high cellularity appeared within the osseous tissue. The tonguelike osseous outgrowths were lined by numerous osteoblasts and smaller numbers of osteoclasts and were surrounded by a fibroblastic reaction of the stroma. Vasculitis was not observed in any of the sections. The mild and infrequent tail lesions in the gelatinase B–deficient mice represented the initial stage of the histopathological evolution and can macroscopically be best compared with an exfoliation or an erosion. In some instances, these lesions were exsudative or mildly bleeding. These never resulted in complete skin ulceration or tail amputation.

Discussion

Gelatinase B has been associated with the pathogenesis and/or development of MS, as well as EAE (19). However, the pathogenic role of gelatinase B has never been proved. Indeed, specific inhibitory mAb's against (mouse) gelatinase B are not available for testing in EAE. Knockout technology offers an elegant alternative to study the effect of gelatinase B. In this study, a phenotype of resistance to EAE development was observed to be limited to young gelatinase B–deficient mice of less than 4 weeks of age. The incidence of disease and the mean disease score were significantly lower in young gelatinase B–deficient animals versus controls. In 2 other studies with gelatinase B–deficient mice, the phenotypic changes were also observed in young mice. Abnormal bone formation was seen in 2- to 4-week-old mice (4), whereas a model of bullous pemphigoid was used in neonatal mice (50). However, in the latter study, no parametric comparisons were done with adult animals. The phenotypic changes in 3- to 4-week-old mice, observed in our experiments, illustrate the importance of gelatinase B function in the postnatal period. It was therefore crucial to know whether lack of gelatinase B was compensated for in adult life. In our mouse EAE model, no differences in mortality, incidence, mean day of onset, and mean disease score were observed in adult gelatinase B–deficient versus control mice. The histopathological findings corroborated the clinical data and suggest the action of alternative or compensatory pathways by other enzymes, as was also observed in the remodeling of the postpartum uterus (51). For instance, matrilysin (MMP-7) or metallo-elastase (MMP-12) might be important enzymes in damaging the CNS in MS (14) and EAE (45).

We also quantified the influx of polymorphonuclear cells in young and adult mice. When the EAE disease was at its height, young gelatinase B–deficient mice showed a significant reduction in infiltrated neutrophils in comparison to controls. This observation was not made in the adult animals. Significant differences in polymorphonuclear myeloperoxidase activity after 12 hours in neonatal knockout versus wild-type mice were previously also noticed in a model of bullous pemphigoid by Liu et al. (50). In our experiments, mononuclear cells were equally distributed in knockout and control animals, both in the young and adult ones. Finally, our study shows that absence of gelatinase B does not preclude destruction of the blood-brain barrier. However, the barrier permeability in young gelatinase B–deficient mice is less affected than in adult, as could be deduced from the

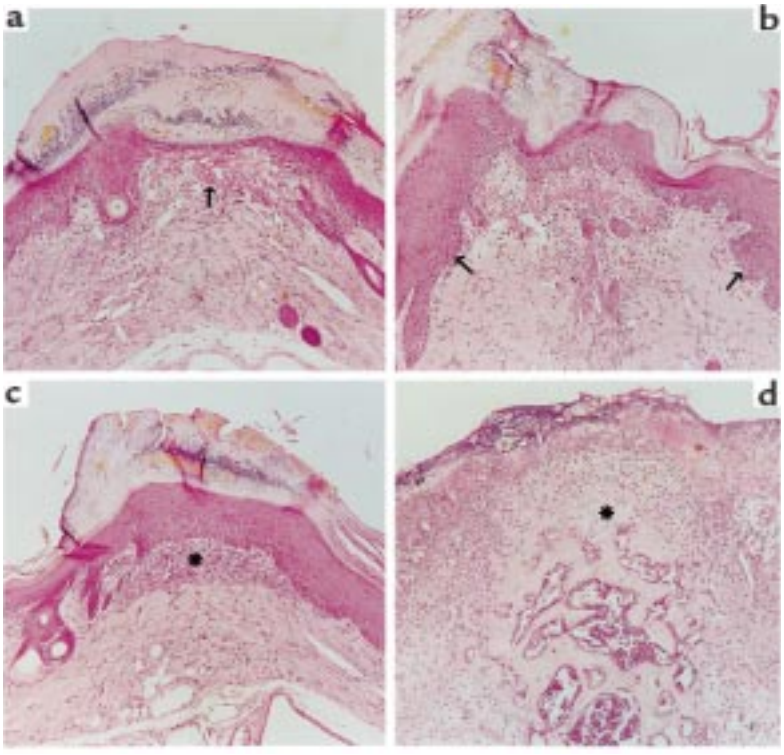

Figure 5
Histopathological findings on the tail lesions in wild-type animals suffering from EAE. (**a**) In the earliest stage fibrinoid material (→) appears immediately underneath the thinned epithelium. Inflammatory cells are present in the overlying horny layer. (**b**) Next, the adjacent epithelium shows irregular hyperplasia (→). (**c**) At the periphery of the lesion a fibroblastic reaction (*) occurs in the dermis. (**d**) Irregular outgrowth of osteocartilaginous tissue (*) occurs when the epithelium is completely ulcerated. Hematoxylin and eosin stain; all panels, ×110.

absence of significant differences for the ratio diseased KO/control KO in Table I. This finding is consistent with our clinical data of EAE disease.

Of the 5 MMPs that have been knocked out, namely MMP-12 (52), MMP-2 (53–54), MMP-7 (55), MMP-9 (4, 50, and this study), MMP-3 (56), none have been lethal to embryos, despite their potentially important roles in development, and several explanations have been proposed to explain lack of expected phenotypes (57). We were able to document the development of compensatory mechanisms during ontogenesis by comparison of EAE between adult and 3- to 4-week-old mice.

Another remarkable observation in this study was the appearance of necrotizing tail lesions with bone hyperplasia in the wild-type mice, whereas the gelatinase B–deficient mice were resistant to this pathology. Our observations extend those of Vu et al. (4), who demonstrated differences in osteocartilaginous tissue between wild-type animals and gelatinase B–deficient animals at young age. As anticipated by its role in remodeling of extracellular matrices, and in particular of collagen types, gelatinase B is a crucial enzyme in bone formation and metabolism. In view of the fact that gelatinase B has been supposed to function in blood vessel remodeling (15), it is tempting to associate the necrotizing lesions to vascular pathology. However, and because there were no clear signs of vasculitis, there exist alternative explanations for this pathology. For instance, the susceptibility for EAE and tail lesion development may be indirectly associated. Indeed, exclusively neurologically affected mice developed this necrosis. Which element or combination of agents of the immunization protocol might play a role in the development of the tail lesions will be the subject of further studies. In acute EAE protocols in SJL/J mice (n = 103) and in 129SvEv (n = 47), the aforementioned tail lesions were not observed.

Because the expression levels of 2 induced phenotypes (EAE and tail necrosis) were clinically followed, we were able to show that in gelatinase B–deficient mice, 1 phenotype (EAE) was compensated for, but the resistance to develop tail lesions remained through ontogenesis. This does not necessarily mean that gelatinase B is not important in adult EAE, rather, it means that other mediators may subserve its function when it is deleted for the life of the mouse (58). In addition, our study shows that gelatinase B is a causative, but replaceable, link in CNS inflammation and therefore that the development of gelatinase B or general MMP inhibitors might be important in the fight against diseases such as MS or those with pathological bone remodeling. Finally, the concept that regulation of extracellular protease–inhibitor balances is involved in autoimmunity (19) is now proved in vivo for 1 specific anticipated MMP family member, gelatinase B.

Acknowledgments

The authors appreciate the excellent technical help of S. Schmitt, J. Weik, G. Küblbeck, C. Dillen, P. Fiten, and M. Groenen and thank P.M. Rudd (Oxford University), A. Billiau, and J. Van Damme (University of Leuven) for critical reading of the manuscript. Helpful discussions with Z. Werb (University of California–San Francisco, San Francisco, California, USA) and V.W. Yong (University of Calgary, Alberta, Canada) are appreciated. This work was supported by the Cancer Foundation of the General Savings and Retirement Fund, the Geconcerteerde Onderzoeksacties, the Scientific Foundation for Multiple Sclerosis Research (Belgium, program 1998–2002), the Fund for Scientific Research (Vlaanderen), the Deutsche Forschungsgemeinschaft (SFB 405, EU BIO4-CT-96007) and the VW-Foundation (I/72-422). Bénédicte Dubois is a research assistant of the Fund for Scientific Research.

1. Agren, M.S., Jorgensen, L.N., Andersen, M., Viljanto, J., and Gottrup, F. 1998. Matrix metalloproteinase 9 level predicts optimal collagen deposition during early wound repair in humans. *Br. J. Surg.* **85**:68–71.
2. Tsafriri, A. 1995. Ovulation as a tissue remodelling process. Proteolysis and cumulus expansion. *Adv. Exp. Med. Biol.* **377**:121–140.
3. Sharkey, M.E., Adler, R.R., Nieder, G.L., and Brenner, C.A. 1996. Matrix metalloproteinase expression during mouse peri-implantation development. *Am. J. Reprod. Immunol.* **36**:72–80.
4. Vu, T.H., et al. 1998. MMP-9/Gelatinase B is a key regulator of growth plate angiogenesis and apoptosis of hypertrophic chondrocytes. *Cell.* **93**:411–422.
5. Vu, T.H., and Werb, Z. 1998. Gelatinase B: structure, regulation, and function. In *Matrix metalloproteinases.* W.C. Parks and R.P. Mecham, editors. Academic Press. San Diego, CA. 115–137.
6. Hua, J., and Muschel, R.J. 1996. Inhibition of matrix metalloproteinase 9 expression by a ribozyme blocks metastasis in a rat sarcoma model system. *Cancer Res.* **56**:5279–5284.
7. van den Oord, J.J., Paemen, L., Opdenakker, G., and de Wolf-Peeters, C. 1997. Expression of gelatinase B and the extracellular matrix metalloproteinase inducer EMMPRIN in benign and malignant pigment cell lesions of the skin. *Am. J. Pathol.* **151**:665–670.
8. Opdenakker, G., Masure, S., Grillet, B., and Van Damme, J. 1991. Cytokine-mediated regulation of human leukocyte gelatinases and role in arthritis. *Lymphokine Cytokine Res.* **10**:317–324.
9. Makela, M., Salo, T., Uitto, V.J., and Larjava, H. 1994. Matrix metalloproteinases (MMP-2 and MMP-9) of the oral cavity: cellular origin and relationship to periodontal status. *J. Dent. Res.* **73**:1397–1406.
10. Gijbels, K., Masure, S., Carton, H., and Opdenakker, G. 1992. Gelatinase in the cerebrospinal fluid of patients with multiple sclerosis and other inflammatory neurological disorders. *J. Neuroimmunol.* **41**:29–34.
11. Paemen, L., Olsson, T., Söderström, M., Van Damme, J., and Opdenakker, G. 1994. Evaluation of gelatinases and IL-6 in the cerebrospinal fluid of patients with optic neuritis, multiple sclerosis and other inflammatory neurological diseases. *Eur. J. Neurol.* **1**:55–63.
12. Maeda, A., and Sobel, R.A. 1996. Matrix metalloproteinases in the normal human central nervous system, microglial nodules, and multiple sclerosis lesions. *J. Neuropathol. Exp. Neurol.* **55**:300–309.
13. Cuzner, M.L., et al. 1996. The expression of tissue-type plasminogen activator, matrix metalloproteases and endogenous inhibitors in the central nervous system in multiple sclerosis: comparison of stages in lesion evolution. *J. Neuropathol. Exp. Neurol.* **55**:1194–1204.
14. Cossins, J.A., et al. 1997. Enhanced expression of MMP-7 and MMP-9 in demyelinating multiple sclerosis lesions. *Acta Neuropathol.* **94**:590–598.
15. Galis, Z.S., Sukhova, G.K., Lark, M.W., and Libby, P. 1994. Increased expression of matrix metalloproteinases and matrix degrading activity in vulnerable regions of human atherosclerotic plaques. *J. Clin. Invest.* **94**:2493–2503.
16. Backstrom, J.R., Lim, G.P., Cullen, M.J., and Tökés, Z.A. 1996. Matrix metalloproteinase-9 (MMP-9) is synthesized in neurons of the human hippocampus and is capable of degrading the amyloid-β peptide (1-40). *J. Neurosci.* **16**:7910–7919.
17. Paemen, L., et al. 1997. Induction of gelatinase B and MCP-2 in baboons during sublethal and lethal bacteraemia. *Cytokine.* **9**:412–415.
18. Murphy, G., and Docherty, A.J.P. 1992. The matrix metalloproteinases and their inhibitors. *Am. J. Respir. Cell Mol. Biol.* **7**:120–125.
19. Opdenakker, G., and Van Damme, J. 1994. Cytokine-regulated proteases in autoimmune diseases. *Immunol. Today.* **15**:103–107.
20. Werb, Z. 1997. ECM and cell surface proteolysis: regulating cellular ecology. *Cell.* **91**:439–442.
21. Van Wart, H.E., and Birkedal-Hansen, H. 1990. The cysteine switch: a principle of regulation of metalloproteinase activity with potential applicability to the entire matrix metalloproteinase gene family. *Proc. Natl. Acad. Sci. USA.* **87**:5578–5582.

22. Cuzner, M.L., and Opdenakker, G. 1999. Plasminogen activators and matrix metalloproteases, mediators of extracellular proteolysis in inflammatory demyelination of the central nervous system. *J. Neuroimmunol.* **94**:1–14.
23. Masure, S., Proost, P., Van Damme, J., and Opdenakker, G. 1991. Purification and identification of 91-kDa neutrophil gelatinase. Release by the activating peptide interleukin-8. *Eur. J. Biochem.* **198**:391–398.
24. Wuyts, A., et al. 1996. Identification of mouse granulocyte chemotactic protein-2 from fibroblasts and epithelial cells. Functional comparison with natural KC and macrophage inflammatory protein-2. *J. Immunol.* **157**:1736–1743.
25. Johnatty, R.N., et al. 1997. Cytokine and chemokine regulation of proMMP-9 and TIMP-1 production by human peripheral blood lymphocytes. *J. Immunol.* **158**:2327–2333.
26. Pagenstecher, A., Stalder, A.K., Kincaid, C.L., Shapiro, S.D., and Campbell, I.L. 1998. Differential expression of matrix metalloproteinase and tissue inhibitor of matrix metalloproteinase genes in the mouse central nervous system in normal and inflammatory states. *Am. J. Pathol.* **152**:729–741.
27. Mazzieri, R., et al. 1997. Control of type IV collagenase activity by components of the urokinase-plasmin system: a regulatory mechanism with cell-bound reactants. *EMBO J.* **16**:2319–2332.
28. Lijnen, H.R., Silence, J., Van Hoef, B., and Collen, D. 1998. Stromelysin-1 (MMP-3)-independent gelatinase expression and activation in mice. *Blood.* **91**:2045–2053.
29. Yong, V.W., Krekoski, C.A., Forsyth, P.A., Bell, R., and Edwards, D.R. 1998. Matrix metalloproteinases and diseases of the CNS. *Trends Neurosci.* **21**:75–80.
30. Proost, P., Van Damme, J., and Opdenakker, G. 1993. Leukocyte gelatinase B cleavage releases encephalitogens from human myelin basic protein. *Biochem. Biophys. Res. Commun.* **192**:1175–1181.
31. Gijbels, K., et al. 1993. Gelatinase B is present in the cerebrospinal fluid during experimental autoimmune encephalomyelitis and cleaves myelin basic protein. *J. Neurosci. Res.* **36**:432–440.
32. Chandler, S., et al. 1995. Matrix metalloproteinases degrade myelin basic protein. *Neurosci. Lett.* **201**:223–226.
33. Leppert, D., Waubant, E., Galardy, R., Bunnett, N.W., and Hauser, S.L. 1995. T cell gelatinases mediate basement membrane transmigration in vitro. *J. Immunol.* **154**:4379–4389.
34. Rosenberg, G.A., Dencoff, J.E., Correa, N., Reiners, M., and Ford, C.C. 1996. Effect of steroids on CSF matrix metalloproteinases in multiple sclerosis: relation to blood–brain barrier injury. *Neurology.* **46**:1626–1632.
35. Schönbeck, U., Mach, F., and Libby, P. 1998. Generation of biologically active IL-1β by matrix metalloproteinases: a novel caspase-1–independent pathway of IL-1β processing. *J. Immunol.* **161**:3340–3346.
36. Paemen, L., Martens, E., Masure, S., and Opdenakker, G. 1995. Monoclonal antibodies specific for natural human neutrophil gelatinase B used for affinity purification, quantitation by two-site ELISA and inhibition of enzymatic activity. *Eur. J. Biochem.* **234**:759–765.
37. Wekerle, H., Kojima, K., Lannes-Vieira, J., Lassman, H., and Linington, C. 1994. Animal models. *Ann. Neurol.* **36**:S47–S53.
38. Swanborg, R.H. 1995. Experimental autoimmune encephalomyelitis in rodents as a model for human demyelinating disease. *Clin. Immunol. Immunopathol.* **77**:4–13.
39. Kieseier, B.C., et al. 1998. Matrix metalloproteinase-9 and -7 are regulated in experimental autoimmune encephalomyelitis. *Brain.* **121**:159–166.
40. Brosnan, C.F., Cammer, W., Norton, W.T., and Bloom, B.R. 1980. Proteinase inhibitors suppress the development of experimental allergic encephalomyelitis. *Nature.* **285**:235–237.
41. Inuzuka, T., Sato, S., Baba, H., and Miyatake, T. 1988. Suppressive effect of camostat mesilate (FOY 305) on acute experimental allergic encephalomyelitis (EAE). *Neurochem. Res.* **13**:225–228.
42. Gijbels, K., Galardy, R.E., and Steinman, L. 1994. Reversal of experimental autoimmune encephalomyelitis with a hydroxamate inhibitor of matrix metalloprotease. *J. Clin. Invest.* **94**:2177–2182.
43. Hewson, A.K., Smith, T., Leonard, J.P., and Cuzner, M.L. 1995. Suppression of experimental allergic encephalomyelitis in the Lewis rat by the matrix metalloproteinase inhibitor Ro31-9790. *Inflamm. Res.* **44**:345–349.
44. Norga, K., et al. 1995. Prevention of acute autoimmune encephalomyelitis and abrogation of relapses in murine models of multiple sclerosis by the protease inhibitor D-penicillamine. *Inflamm. Res.* **44**:529–534.
45. Clements, J.M., et al. 1997. Matrix metalloproteinase expression during experimental autoimmune encephalomyelitis and effects of a combined matrix metalloproteinase and tumour necrosis factor-α inhibitor. *J. Neuroimmunol.* **74**:85–94.
46. Leppert, D., Waubant, E., Bürk, M.R., Oksenberg, J.R., and Hauser, S.L. 1996. Interferon beta-1b inhibits gelatinase secretion and in vitro migration of human T cells: a possible mechanism for treatment efficacy in multiple sclerosis. *Ann. Neurol.* **40**:846–852.
47. Stüve, O., et al. 1996. Interferon β-1b decreases the migration of T lymphocytes in vitro: effects on matrix metalloproteinase-9. *Ann. Neurol.* **40**:853–863.
48. Masure, S., Nys, G., Fiten, P., Van Damme, J., and Opdenakker, G. 1993. Mouse gelatinase B. cDNA cloning, regulation of expression and glycosylation in WEHI-3 macrophages and gene organisation. *Eur. J. Biochem.* **218**:129–141.
49. Baker, D., O'Neill, J.K., Davison, A.N., and Turk, J.L. 1992. Control of immune-mediated disease of the central nervous system requires the use of a neuroactive agent: elucidation by the action of mitoxantrone. *Clin. Exp. Immunol.* **90**:124–128.
50. Liu, Z., et al. 1998. Gelatinase B–deficient mice are resistant to experimental bullous pemphigoid. *J. Exp. Med.* **188**:475–482.
51. Rudolph-Owen, L.A., Hulboy, D.L., Wilson, C.L., Mudgett, J., and Matrisian, L.M. 1997. Coordinate expression of matrix metalloproteinase family members in the uterus of normal, matrilysin-deficient, and stromelysin-1–deficient mice. *Endocrinology.* **138**:4902–4911.
52. Shipley, J.M., Wesselschmidt, R.L., Kobayashi, D.K., Ley, T.J., and Shapiro, S.D. 1996. Metalloelastase is required for macrophage-mediated proteolysis and matrix invasion in mice. *Proc. Natl. Acad. Sci. USA.* **93**:3942–3946.
53. Itoh, T., et al. 1997. Unaltered secretion of β-amyloid precursor protein in gelatinase A (matrix metalloproteinase 2)-deficient mice. *J. Biol. Chem.* **272**:22389–22392.
54. Itoh, T., et al. 1998. Reduced angiogenesis and tumor progression in gelatinase A–deficient mice. *Cancer Res.* **58**:1048–1051.
55. Wilson, C.L., Heppner, K.J., Labosky, P.A., Hogan, B.L.M., and Matrisian, L. 1997. Intestinal tumorigenesis is suppressed in mice lacking the metalloproteinase matrilysin. *Proc. Natl. Acad. Sci. USA.* **94**:1402–1407.
56. Mudgett, J.S., et al. 1998. Susceptibility of stromelysin 1–deficient mice to collagen-induced arthritis and cartilage destruction. *Arthritis Rheum.* **41**:110–121.
57. Shapiro, S.D. 1997. Mighty mice: transgenic technology "knock out" questions of matrix metalloproteinase function. *Matrix Biol.* **15**:527–533.
58. Steinman L. 1997. Some misconceptions about understanding autoimmunity through experiments with knockouts. *J. Exp. Med.* **185**:2039–2041.